Comparison of Human Body Models in Frontal Crashes with Reclined Seatback

B. D. Gepner, D. Draper, K. Mroz, R. Richardson, M. Ostling, B. Pipkorn, J. L. Forman, J. R. Kerrigan

Abstract

Reclined seating configurations, relevant to the future of Autonomous Driving Systems is likely to challenge the current state-of-the-art restraint systems. Human body models (HBM) offer an attractive tool to support the design process, however their validity in the reclined scenario remains questionable. The goal of this study is to compare the response of selected HBMs in the frontal, reclined scenario, while utilizing a new prototype restraint system. A sled model with a generic seat, 50 deg seatback recline angle and a prototype 3-point belt system was used in this study. Four different male HBMs were compared, the Global Human Body Model Consortium (GHBMC) simplified occupant model (GHBMC-S), the GHBMC detailed model (GHBMC-D), Total Human Model for Safety SAFER (THUMS-S) model, and THUMS-v5 model. All HBMs showed good pelvis engagement, except GHBMC-D that submarined under the lap belt. Additionally, large differences were observed in pelvis and lumbar spine response between GHBMC and THUMS family models. Since no relevant PMHS data is currently available, it is impossible to evaluate the biofidelity of these models in the reclined scenarios. Evaluating the relative biofidelity of these models can only be accomplished with experimental data capturing detailed 3D skeletal kinematics and all the boundary forces necessary for model evaluation.

Keywords: *Recline, submarining, PMHS, HBM, restraint*

I. INTRODUCTION

The introduction of Autonomous Driving Systems (ADS) is likely to change the nature of personal transportation. With increased automation, the vehicle manufacturers will be enticed to offer new interior configurations, along with new seating arrangement. With the introduction of Level 3 automation, the driver will no longer be required to constantly and actively engage with the vehicle controls [1-3]. This change in vehicle operations is likely to influence the occupant's behavior. As seen in both automotive [4, 5]and aviation industries, the passengers may want to rest during extended travel by reclining their seats and moving it away from the instrument/entertainment panel. However, these seating choices may challenge the ability of current vehicle safety systems to adequately protect the occupants.

Current restraint systems (3 point belt with B-pillar D-ring), developed for the present vehicle interior and tested, for an upright seated occupants may no longer be adequate for the application in the ADS. Previous experimental and computational studies have suggested that the increase in the seatback recline angle leads to an increased risk of submarining, i.e. the lap belt loads the abdominal soft tissues, after passing over the iliac crest of the pelvis without engaging, or after disengaging, the pelvis. This was observed for both, systems without [6], and with lap belt pre-tensioning [7-11]. Additionally, with increase in the recline angle, belt with B-pillar mounted D-ring leads to a delayed torso engagement and increase in forward excursion of the pelvis. This could be partially mitigated by the use of seatback integrated D-ring, but it is not an effective measure to eliminate submarining [6, 10, 11]. Several studies have shown that knee bolster and knee airbags [12] could be an effective countermeasure for controlling occupant kinematics and preventing submarining [7, 8, 13], however it may no longer be available in the ADS occupant environment. This shows that there is a need for a new restraint system that could effectively protect occupants in the ADS relevant environment.

Traditionally, restraint systems were developed and tested using anthropomorphic test devices (ATD), or crash test dummies, intended for specific loading conditions. However, no ATD was developed to evaluate occupant-

B. D. Gepner is a Research Scientist (+1-434-297-8046 / bgepner@virginia.edu), R. Richardson is a PhD student in Mechanical Engineering, J. L. Forman is a Principal Scientist, J. R. Kerrigan is an Assistant Professor of Mechanical and Aerospace Engineering at University of Virginia, USA. D. Draper is a PhD student in Mechanical Engineering at Ludwig Maximilian University of Munich, K. Mroz, M. Ostling are Reserchers at Autoliv Research, Vårgårda, Sweden and B. Pipkorn is Adjunct Professor at Chalmers University of Technology and Director of Simulation and Active Structures at Autoliv Research.

restraint interaction in conditions with high level of seatback recline. This situation calls for a rapid shift in vehicle and restraint system design. Virtual tools, such as human body models (HBM) offer an attractive tool to support the design process. National Highway Traffic Safety Administration (NHTSA) has recently acknowledged that future design of countermeasures need not to be limited to physical ATD testing but also could include virtual tests using available HBMs [2]. In [3] NHTSA additionally stated that Federal law does not require that NHTSA's safety standards rely on physical tests and measurements, indicating a possibility for future virtual compliance tests. However, similar to the ATDs, HBMs have limitations and remain relevant only within their development and validation regime. Currently, two families of HBMs are widely used by the injury biomechanics community. Total Human Model for Safety (THUMS) developed by Toyota, and Global Human Body Model Consortium (GHBMC) developed by the consortium of several automotive companies and NHTSA. Even though these models were developed and validated for variety of impact scenarios their applicability is limited to traditional seating environment without considering reclined occupants. Moreover, until recently, no post mortem human subject (PMHS) validation data was available for reclined occupants, with the exception of one recently published study [14].

The goal of this study was to compare the performance of available HBMs in the frontal, reclined scenario, utilizing a new prototype restraint system designed to eliminate submarining. The specific goal of this study was to understand the discrepancies in HBMs response, resulting from their use outside validation regime. This was accomplished by utilizing four different 50th male HBMs, in sled environment matching the one used in the recent reclined PMHS test series. The information from this study may be used inform the future of component bio-fidelity and validation experiments.

II. METHODS

The simulation environment was developed following the setup used in the recently completed reclined, full body, PMHS test series [14]. [14] used a previously developed semi-rigid simplified seat, a 50 deg. torso recline angle, and a prototype seatback integrated 3-point restraint system. No knee bolster was used in this study.

Seat model

The semi-rigid seat used in [14] was based on a design developed by [15] and previously used in several PMHS studies [15, 16]. The seat consists of two adjustable articulated plates that can be individually configured in geometry and spring stiffness response to match a specific production seat. In [15] the stiffness of the springs was set to represent a front seat configuration. The seat pan was angled at 15 deg. and the anti-submarining ramp was angled at 30 deg from the horizontal. Upon deflection of the articulated plates, an anti-rebound locking mechanism was engaged to reduce the level of elastic energy returned into the subject by the seat on rebound. The Finite Element (FE) model of the semi-rigid seat developed by LAB/CEESAR in cooperation with PDB was further developed in-house for the specific purpose of this study. The model consists of rigid geometrical representation of plate structures, interconnected by a series of joints, springs and dampers to facilitate appropriate model response (Fig. 1). The modelling of the seat and anti-submarining ramp spring systems were updated, and a new lower frame was developed to facilitate the use of a three load cell configuration below the seat. The seat pan was shortened by app. 20mm to allow for a longer seat pan stroke by avoiding interaction to the anti-submarining pan. The modified seat model was finally validated in static loading against moment-rotation responses published in [15].

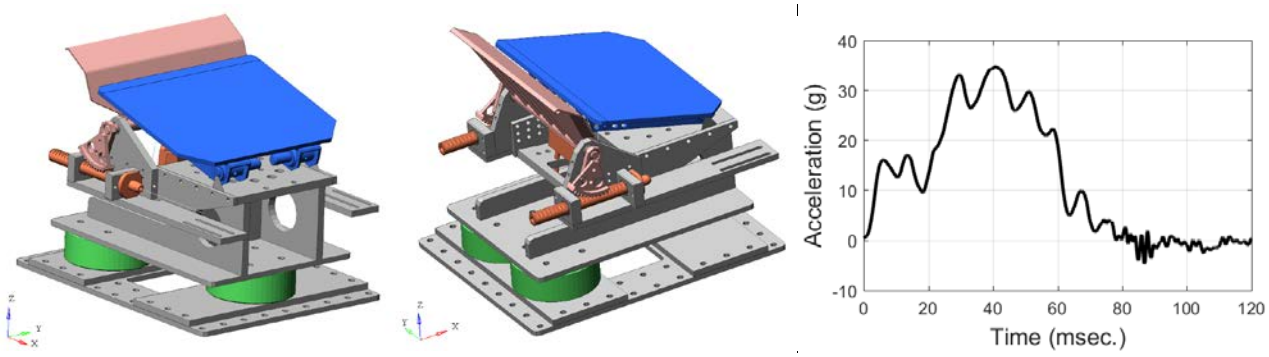

Fig. 1. FE model of LAB Seat developed by LAB/CEESAR in cooperation with PDB (left). Full frontal rigid barrier pulse 50 km/h (right).

Pulse

A 50 km/h full frontal rigid barrier pulse with a peak acceleration of 35g and a delta-v of 51km/h [14-16] was used in this study (Fig. 1).

Restraint system

The belt system used in this study was designed to increase engagement of the pelvis, reducing the risk of submarining for reclined occupants. This consisted of a 3-point belt equipped with dual lap-belt pretensioners and a shoulder-belt retractor pretensioner. The inboard lap pretensioner was activated at 3ms and the remaining two pretensioners at 9ms. Additionally, the belt system included a crash locking tongue that obstructed webbing transport from shoulder-belt to lap-belt and a shoulder-belt load limiter of approximately 3.5 kN. The D-ring was positioned to simulate the approximate position of a seatback-integrated D-ring, with a belt angle of approximately 12 deg as the belt leaves the shoulder. The shoulder belt crossed the shoulder at approximately mid-clavicle. The FE model of the restraint system was developed using shell seatbelt element and 2D slip-rings formulation to facilitate stable and unobstructed belt payout. In-house validated component models of the pretensioners and retractors which closely match those of the mechanical counterparts were used in the belt system.

HBMs

Four different 50th percentile male HBMs were compared in this study, the GHBMC simplified occupant model (GHBMC-S) version 1.8.4, the GHBMC detailed model (GHBMC-D) version 4.5, THUMS SAFER model version 9 (THUMS-S), and THUMS version 5 model (THUMS-V5).

The simplified GHBMC model was developed as a tool designed to capture kinetics and kinematics, without a need to execute a full and expensive detailed GHBMC model. The model was constructed by simplifying an existing GHBMC model, using simplified material models, rigid bones, discrete joints and simplified, homogenized internal organs. Consequently, the simplified GHBMC model shares several modeling features, as well as the skeletal and external geometry with the detailed GHBMC model [17]. Both GHBMC models required several changes from their original release configuration to both improve model stability, and address several modeling inconsistencies discovered in the previous studies [7, 8]. Changes to the GHBMC-S model included correcting lumbar spine polarity definition, modifying contacts, changes in the sacroiliac (SI) joint material properties. In GHBMC-D model the hourglass definition was updated to improve its robustness in severe loading conditions.

The THUMS-S model was developed from THUMS version 3 by modifications to the chest geometry, rib cortical bone thickness and properties (Appendix A) [18]. The lumbar spine vertebrae were remeshed and the intervertebral ligaments were modified with respect to geometry and properties. Contact between vertebra and intervertebral disk was also added. Also, a new head model was implemented to the THUMS-S HBM. The THUMS-v5 was also developed from THUMS version 3. The modifications included changes in long bone models in the lower extremities, thoracic and lumbar spines, shoulder, internal organs, addition of whole body muscles and an improved head model [19].

Positioning

Since no detailed occupant positioning information was available from [14] at the time of this publication all HBMs were positioned to match the approximated PMHS positions using initial data from the external retroreflective body markers. However, care was taken to match the occupant positioning between all tested HBMs. Since the two model families differed in specific bony geometry, the positioning was carried out by matching several selected anatomical landmarks. This allowed for matched occupant positions without forcing the evaluated HBMs into over-constrained positions. First, since pelvis to belt interaction was at the center of this study, the pelvis position was matched across all used HBMs. This was achieved by aligning the pelvis reference plane formed by the right and left anterior superior iliac spine (ASIS) and pubic tubercle (PT), as defined by [20] (Fig. 2). Second, with pelvic bone fixed in place the occupants were positioned to match torso angle (ASIS-Acromion), head position (Head CG), and femur angle. Similarly to the PMHS tests the upper extremities were moved up and away from the torso (Fig. 3).

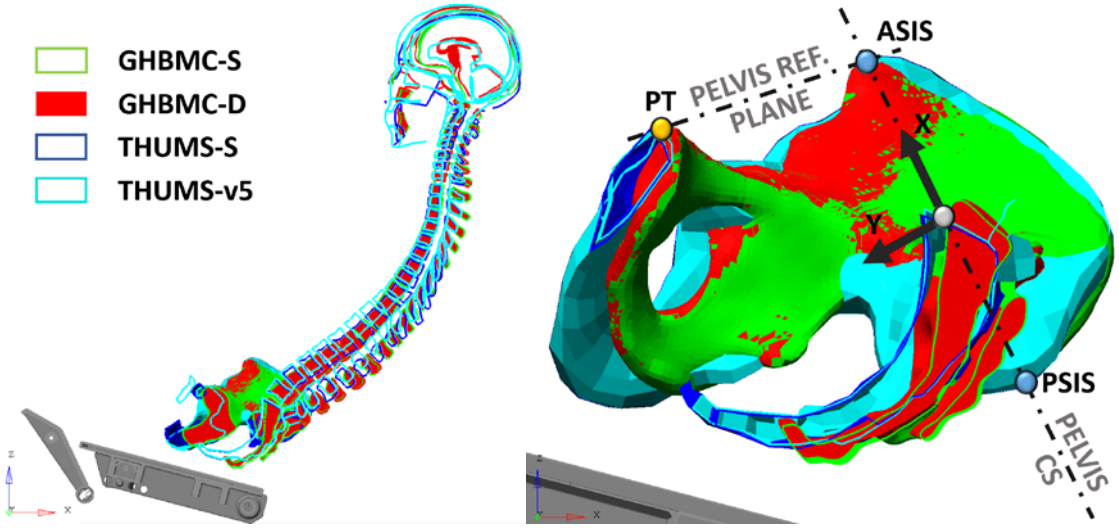

Fig. 2. Comparison of initial HBMs spine (left) and pelvis (right) positions. Pelvis coordinate system and reference plane definition (right).

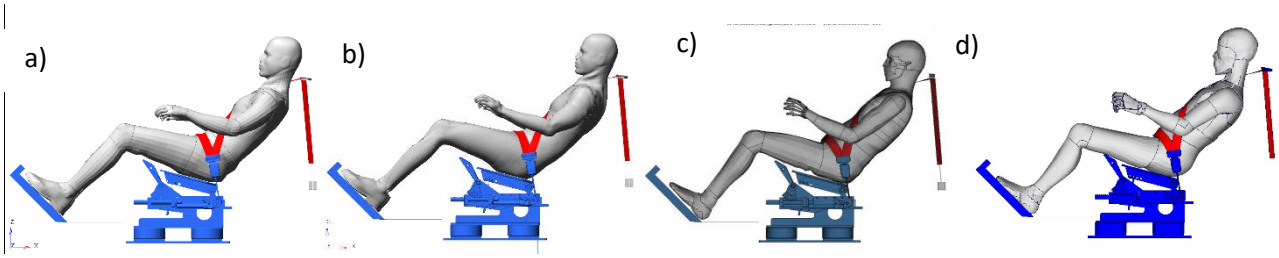

Fig. 3. Initial position of all evaluated HBM, a) GHBMC-S, b) GHBMC-D, c) THUMS-S and d) THUMS-v5.

Data processing

All HBM were evaluated in matching boundary conditions, and all boundary data was extracted uniformly for all evaluated models. However, since the models used different modeling approaches sometimes direct comparison of the response signals was impossible. For THUMS models the lumbar spine forces were extracted from the sectional forces of the individual lumbar vertebral bodies. In both GHBMC models, the lumbar spine is modeled using the zero length discrete beams connecting rigid vertebrae bodies. Discrete beams are used to assign appropriate connectivity and stiffness in each of the six degrees of freedom. For the GHBMC model the force was extracted from the zero length beam below each vertebrae in question.

III. RESULTS

Simulation outcome

All four HBM simulations were scheduled for 120 msec. runtime, however only THUMS-S and GHBMC-D reached normal termination. Both, GHBMC-S and THUMS-v5 terminated prematurely at around 100 msec. Nevertheless, these results provided satisfactory basis for the model performance comparison.

Initial Belt position

Since the belt was allowed to conform to the external flesh outline, its initial position relative to the pelvis varied between the evaluated HBMs. In case of the GHBMC models, the top edge of the belt was both closer horizontally and vertically to the ASIS, then in case of THUMS models. For GHBMC the belt laid horizontally over the pelvis. In case of THUMS models, the belt was more angled relative to the pelvis, with the bottom edge lower and closer to the ASIS (Fig. 3).

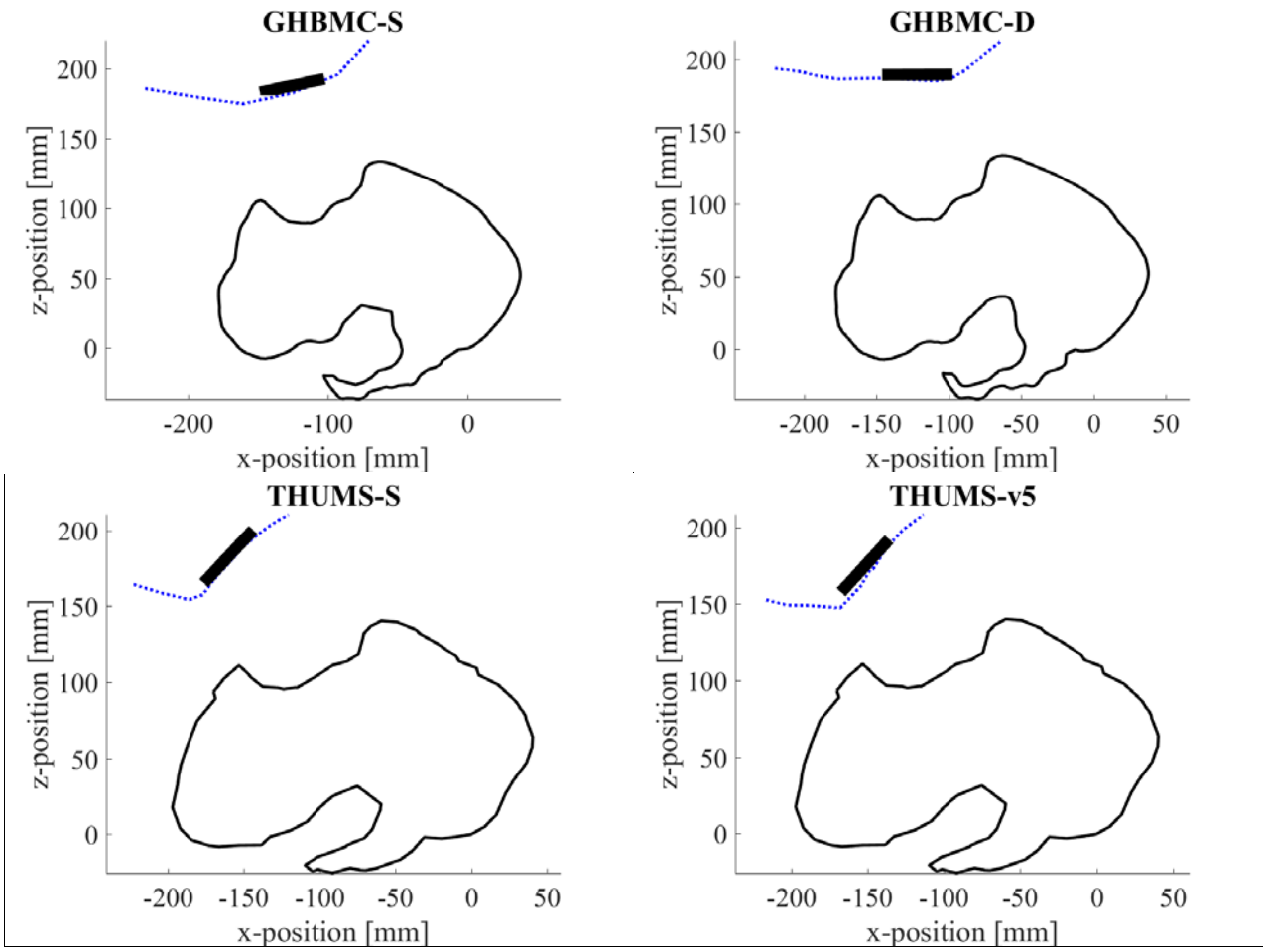

Fig. 4. Initial belt position at the centerline relative to the occupant's pelvis. The outline of occupant flesh shown.

Kinematic

Both THUMS models and the GHBMC-S showed similar kinematics. The lap belt effectively constrained occupant's pelvis, and allowed forward torso motion. The kinematic response looked comparable across all three model at 100 msec. (Fig. 4a,c,d). The GHBMC-D differed from all other models. In this case the model showed pelvis submarining under the lap belt, increased forward pelvis motion, pelvis engagement with the anti-submarining ramp, and limited upper extremity motion (Fig. 4b).

a)

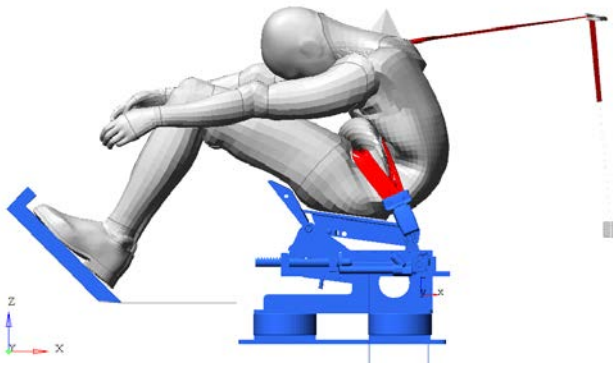

b)

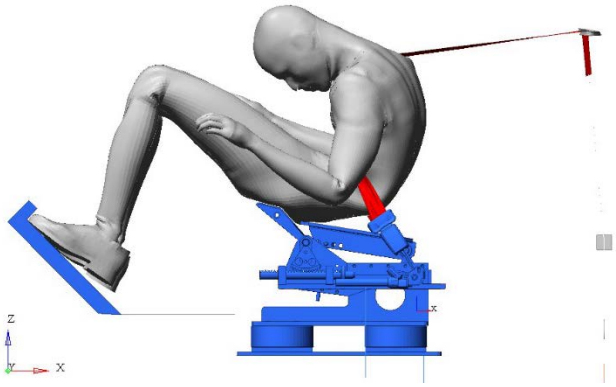

c)

d)

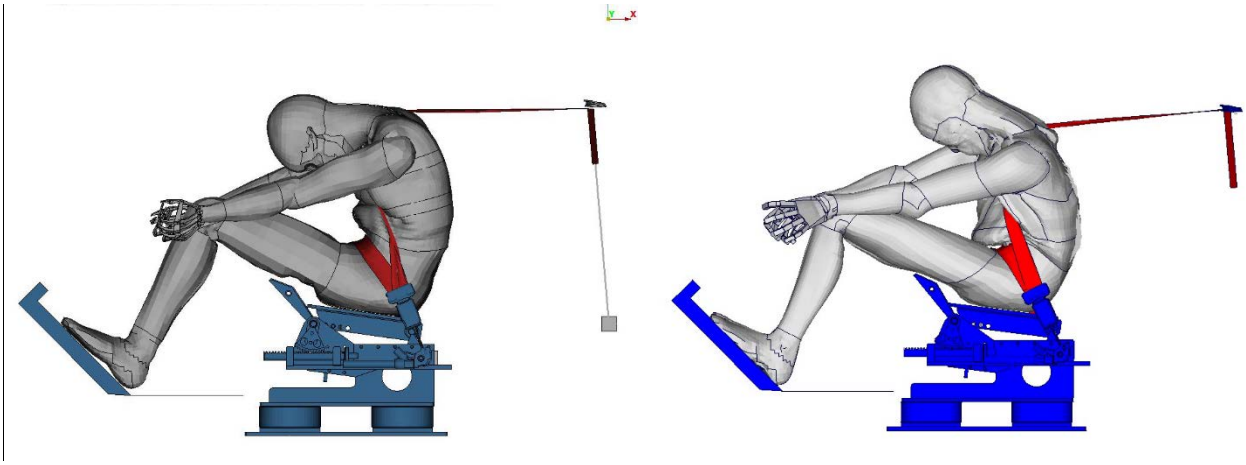

Fig. 5. Still frames extracted from the simulation at 100 msec. a) GHBMC-S, b) GHBMC-D, c) THUMS-S and d) THUMS-v5.

Belt forces

The recorded belt forces were comparable across all models with the exception of the GHBMC-D model. The GHBMC-D models showed much lower lap belt forces. In this case the load measured on both sides of the lap belt showed a sharp drop at 60 msec. associated with the loss of engagement of the pelvis. Additionally, the GHBMC-D model experienced reduction in the recorded shoulder belt force (3 kN) when compared with other HBMs (4kN) (Fig. 5). The reduction in the lap belt force was associated with the GHBMC-D model engagement with the anti-submarining pan which provided additional restraining force.

Both THUMS and GHBMC-S models showed a peak lap belt force ranging from 7 to 8 kN for the buckle side and 8 to 9.5 kN on the anchor side. Interestingly, the THUMS-S showed the highest peak force on both anchor and buckle side of the belt (Fig. 5).

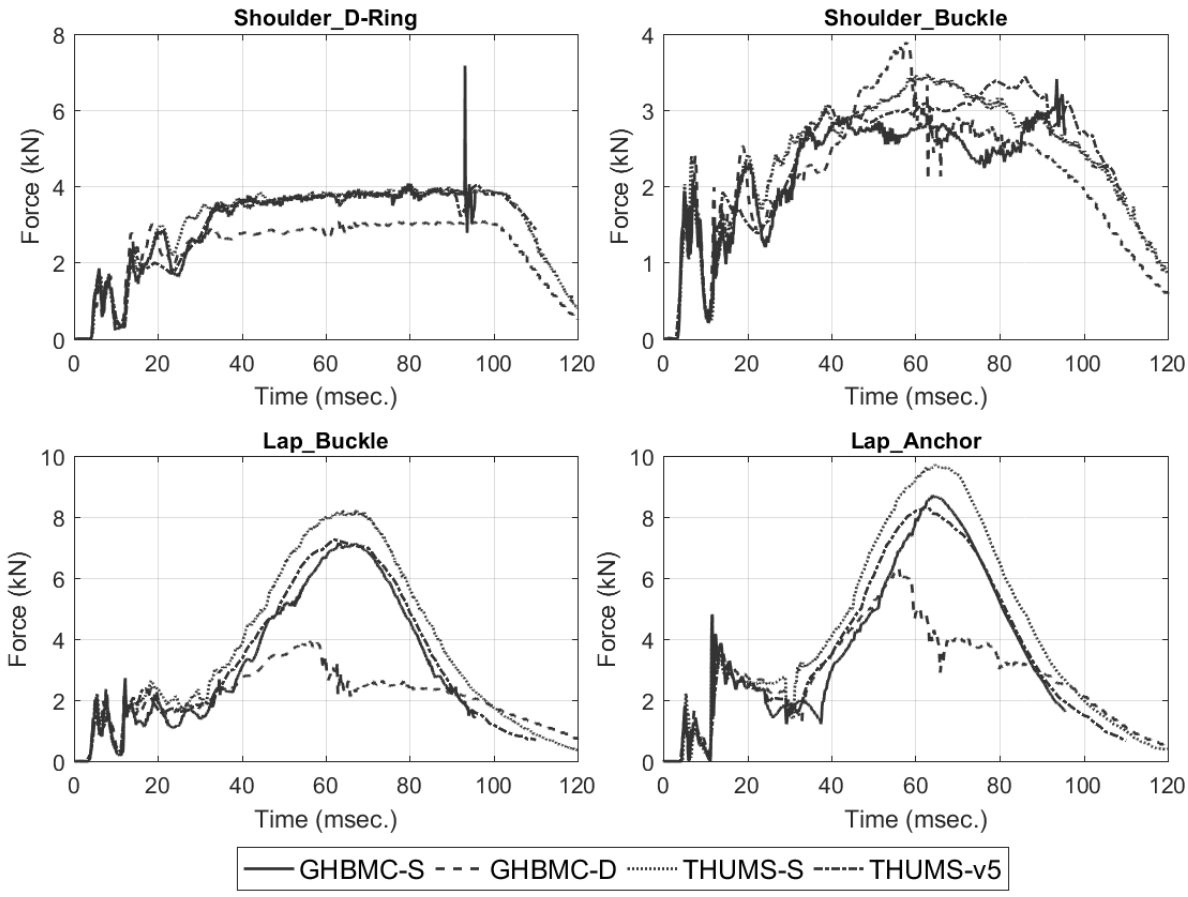

Fig. 6. Cross-sectional belt forces measured for each HBM.

Belt engagement

Both THUMS models and the GHBMC-S showed good pelvis-lap belt engagement (Fig. 6). In these cases the belt remained in front of the ASIS throughout the simulation, effectively limiting pelvis forward motion. In case of the GHBMC-D model the lap belt initially engaged the pelvis at the ASIS, however at 60 msec. it slipped off, passed over the iliac crest and penetrated into the abdomen (Fig. 6).

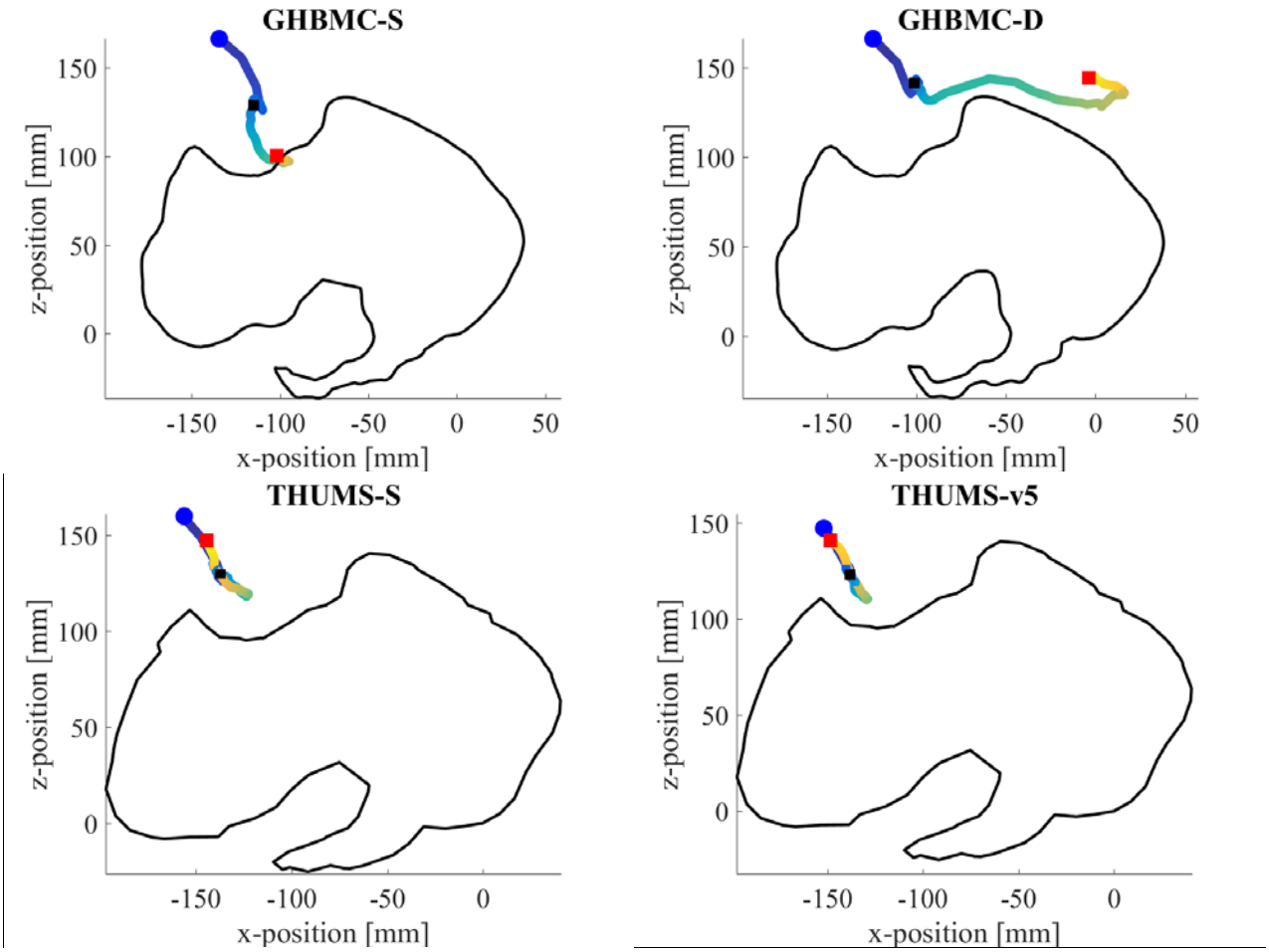

Fig. 7. Trajectory of the lap belt recorded in the pelvis reference frame. For each case a point at the bottom of the lap belt, directly in front of the left iliac wing is shown. Blue circle depicts the belt initial, and red square its final position. Black square depicts a point (20msec.) after both lap belt pretensiones were fully deployed.

Lumbar spine kinematics

The lumbar spine response varied across the two families of evaluated HBMs. The THUMS models, which had similar response, maintained the initial lumbar spine alignment up until 60 msec., after which it progressed into flexion. Additionally, for these models their pelves showed relatively little rotation in sagittal plane and limited pelvis forward excursion (Fig. 8 and Fig. 9).

GHBMC models on the other hand experienced larger pelvis rotation. In both models the pelvis rotated posteriorly during initial lap belt engagement, resulting in the posterior rotation of the lumbar spine. Both GHBMC models differed in the lumbar spine response. While the lumbar spine in the GHBMC-D remained aligned until 60 msec. the GHBMC-S model diverged from its initial alignment past 40 msec. Additionally, towards the end of the simulation the simplified model showed larger lumbar spine flexion when compared to the detailed GHBMC (Fig. 8). The detailed model, on the other hand, showed large pelvis forward excursion which was a consequence of the model submarining under the lap belt.

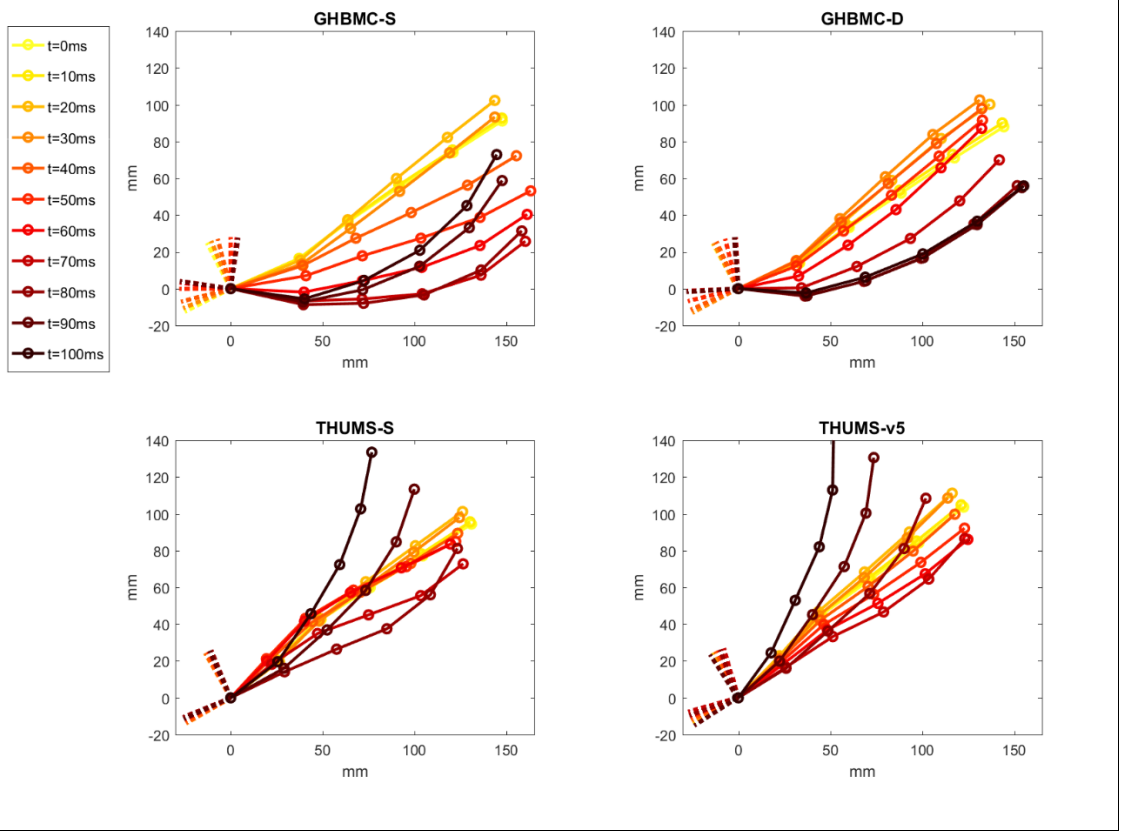

Fig. 8. Lumbar spine (Pelvis - L1) trajectories across all evaluated HBM. All responses were measured relative to the pelvis origin (Fig. 2). Each vertebra is shown as a dot, and X and Z axis of the pelvis coordinate system are shown as dashed lines.

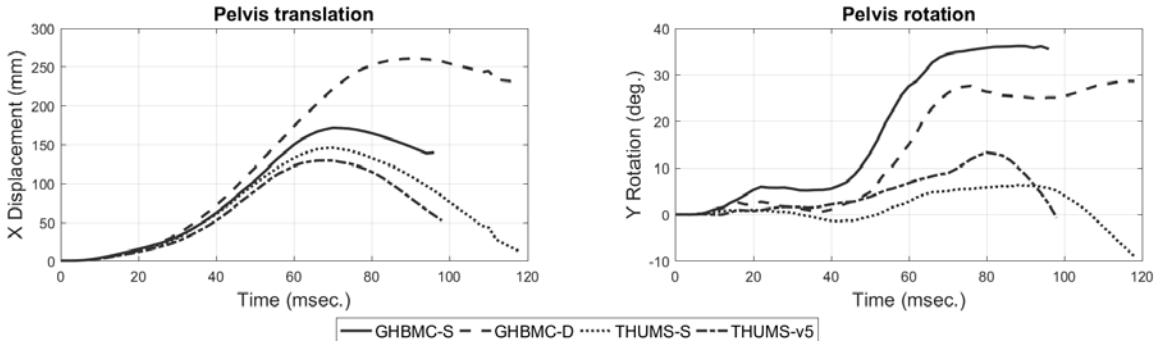

Fig. 9. Pelvis translation relative to the sled in the longitudinal direction (left), and pelvis rotation in the sagittal plane (right). Comparison across all four evaluated models.

Lumbar spine forces

All models showed lumbar spine compression force (Fz) and flexion moment (My), however there were large discrepancies in the level of recorded forces (Fig. 8, Fig. 9, Fig. 10, and Fig. 11). THUMS models were most similar with 4 kN peak compression force and 100 Nm peak flexion moment. Both models showed highest flexion moment in either the L1 or L2 vertebrae. Interestingly these models showed relatively high (25Nm) lateral bending moment (Mx), however, the response appeared inverted with L1 and L5 showing either lowest or highest moment depending on THUMS model.

GHBMC-D recorded highest peak bending moment (400Nm) at 80 msec., however this was observed after the lap belt slipped off the pelvis and the HBM submarined. Submarining was also associated with the increase anterior-posterior (AP) shear force (Fx), not observed in other HBM's. Interestingly, the GHBMC-D model recorded similar level of lumbar spine compression force (4kN) prior to submarining, as the one observed in both THUMS models. GHBMC-S showed the lowest peak compression force (1.5kN) and flexion moment (50 Nm) among all evaluated models.

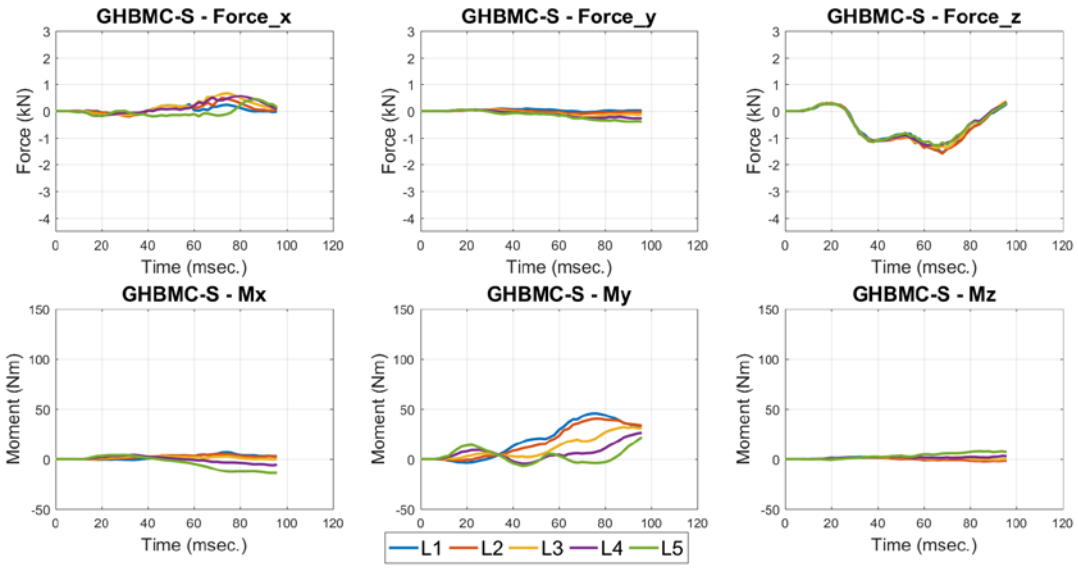

Fig. 10. Lumbar spine forces recorded for the GHBMC-S model.

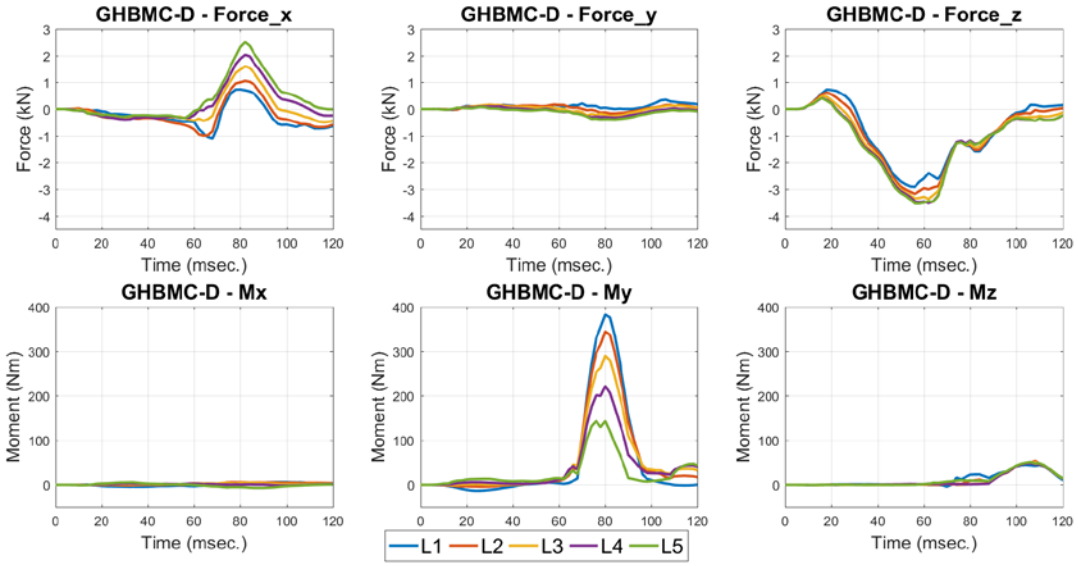

Fig. 11. Lumbar spine forces recorded for the GHBMC-D model with submarining occuring at 60 msec.

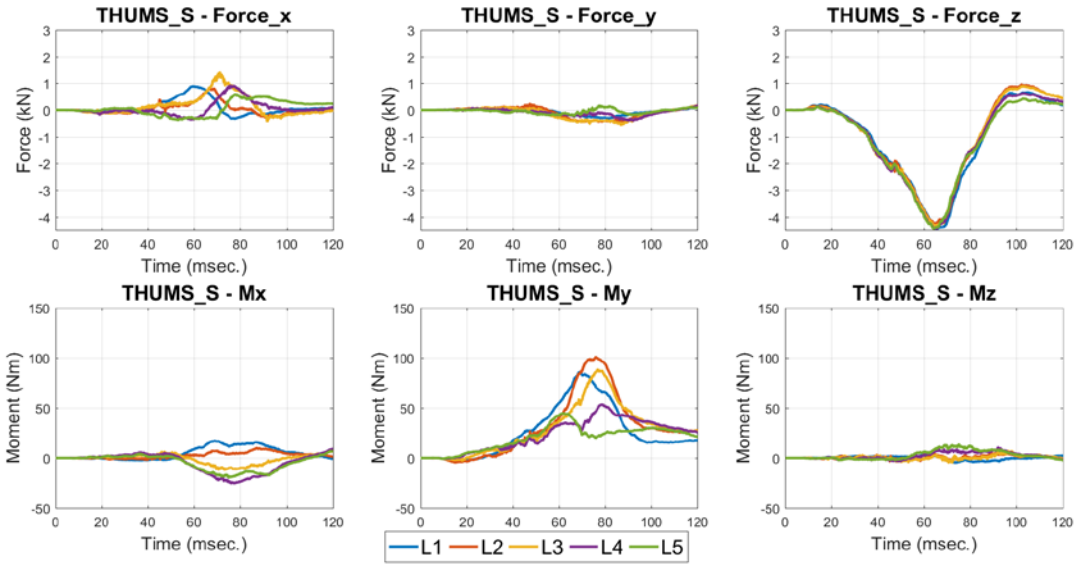

Fig. 12. Lumbar spine forces recorded for the THUMS-S model.

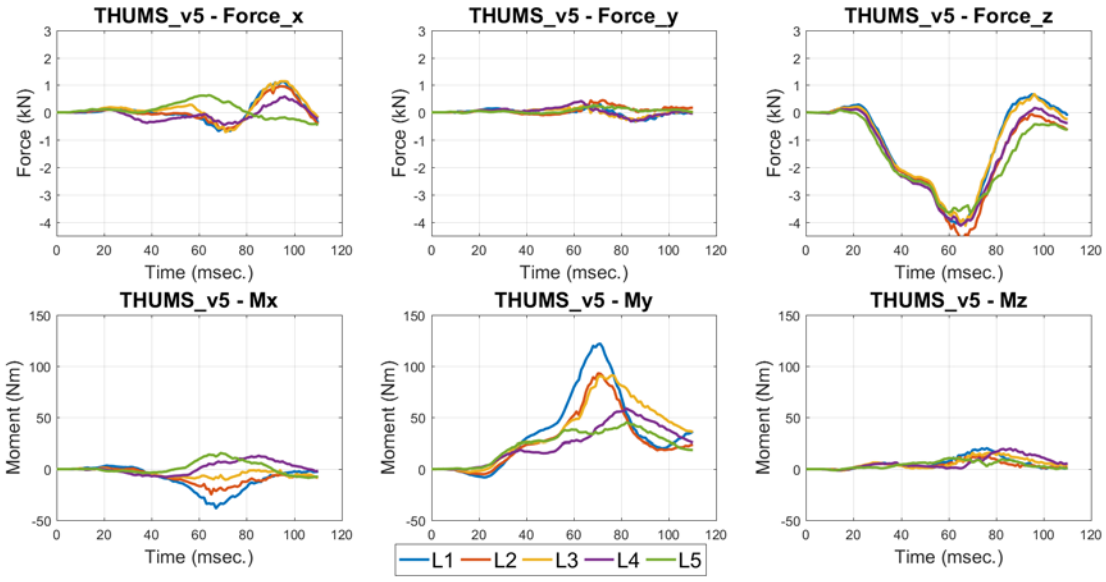

Fig. 13. Lumbar spine forces recorded for the THUMS-v5 model.

IV. DISCUSSION

The results indicate substantial differences in the response of available HBMs when used in a reclined configuration, and additional work is needed to assess the biofidelity of each and to refine those require improvement. The evaluated HBMs showed differing response when tested with matching boundary conditions. The results indicate that at least some of the currently available HBMs still need more work and development to be a trustworthy tools for evaluating occupant safety in ADS environments.

This study utilized four different HBMs with matched pelvis position and torso angle. However, the outline of the external flesh varied from model to model, and lead to a varied lap belt position among tested HBMs. THUMS models had more abdominal tissue located over the pelvis, which lead to belt routing up and away from the ASIS (Fig. 3). This geometrical consideration is important, since initial lap belt placement may influence the ability for the lap belt to engage with the pelvis.

Three out of four evaluated models showed good belt-pelvis engagement throughout the entire simulation. However, the fourth model (GHBMC-D) submarined. Fig. 6 shows the trajectory of the lap belt, as well as lap belt position after deployment of both lap belt pre-tensioners (t = 20 msec). For all other models the lap belt was driven below the ASIS after the pre-tensioners were engaged, however in case of the GHBMC-D model, the belt remained high. The high position of the belt prevented proper pelvic engagement, led to submarining, engagement with the anti-submarining pen and resulted in the lower recorded lap belt forces (Fig. 5).

The fundamental difference between the model that submarined and the models that did not, is within the flesh definition and its attachment to surrounding tissues, and has been previously documented in [8]. Previous studies have shown that current GHBMC flesh definition is too stiff compared to that of humans [21]. This finding was not surprising, given that stiffer formulation is often used to improve the stability of the model in cases where tissue deformation is not critical for model response. Additionally GHBMC-D is the only model that features continuous attachment between the pelvic flesh and the pelvic bone. In all other models the flesh is allowed to move on top of the pubic bone with a sliding style contact. The potential for pelvis-to-flesh sliding, facilitates the low shear boundary condition between the flesh and the bony structure. This allows for more motion between the flesh and the pelvis, and enables the pre-tensioners to drive the lap belt lower below the ASIS. However, due to the continuous definition of the pelvis-flesh construct, and increased flesh stiffness, the pre-tensioner effectiveness is limited in case of GHBMC-D model. This leads to the lap belt remaining above the ASIS, and consequently submarining.

The two families of HBM show large differences in lumbar spine kinematics. The most notable difference is seen in the occupant's pelvis rotation. While GHBMC models showed substantial backwards rotation of the pelvis, there was hardly any rotation recorded for THUMS models (Fig. 8 and Fig. 9). The difference in pelvis rotation had

a big effect on kinematics of the lumbar spine. In case of both GHBMC-S and GHBMC-D (prior to submarining), the backward rotation of the pelvis resulted in rotation of the lumbar spine into more horizontal alignment. For the GHBMC-S model S1-L4 alignment remains unchanged throughout later stages of the simulation, while upper lumbar spine underwent large flexion. THUMS models showed much smaller backward rotation of the pelvis, and consequently almost no backward rotation of the S1-L4 spine section. Both THUMS models maintained initial lumbar spine alignment until 60 msec. after which they both progressed into flexion (Fig. 8).

Recorded lumbar spine forces showed several similarities across all evaluated HBMs (Fig. 8, Fig. 9, Fig. 10, and Fig. 11). Both THUMS models as well as the GHBMC-D showed similar level and timing of peak lumbar spine compression force (4 kN), prior to GHBMC-D submarining at 60 msec. The 4 kN compression force is similar to previously reported 50% of isolated compression injury risk value (4.5 kN) reported previously by [22]. Assuming the validity of these results, it indicates that this configuration could be injurious for the lumbar spine.

GHBMC-S model response was different among all evaluated HBMs with the peak lumbar with a peak compression force at 1.5 kN and peak flexion moment at 50Nm (Fig. 8). Additionally the GHBMC-D model showed a large difference in the peak lumbar spine flexion moment (400 Nm vs. 100 Nm and 50 Nm) which was a result of occupant submarining, where the belt moved over the pelvis and loaded lumbar spine directly resulting in large flexion and AP shear forces (Fig. 9). Interestingly, both THUMS models showed slightly different timing of the peak compression forces and flexion moments. While THUMS-v5 model showed both peak force and moment simultaneously at 65 msec. the THUMS-S model showed a 10 msec. (Fig. 10, Fig. 11) delay between recorded peaks. The timing of each component could be important for the consideration of the possible future combined injury threshold where both compression and flexion components should be considered.

The differences in the lumbar spine forces recorded for all HBMs may be related to the respective lumbar spine model definitions. Both THUMS use contact based models with deformable vertebral bodies and intervertebral discs, with major ligaments included which can be used for refining lumbar spine response (Appendix A), [18, 19]. The GHBMC models, on the other hand, use rigid vertebral bodies interconnected with discrete zero length beams. The zero length beams represent the stiffness of all the structures within the joint and can be modified to match a given biofidelity performance target. The GHBMC-S lumbar spine model was based on the detailed GHBMC model version 4.4. However, the GHBMC-D version 4.5, used for this study, has an updated lumbar spine definition, with modified lumbar spine performance curves, that differs from the one used in the GHBMC-S model. Since the GHBMC-D lumbar performance curves have been modified to include stiffening response past certain deformation, this likely contributes to the higher forces recorded by the GHBMC-D model (Appendix B). Lastly, it needs to be noted that newly released GHBMC version 5.0 model, which was not available for this study, features a fully deformable, contact based lumbar spine, which might address several of the observed discrepancies.

This study provides the comparison among several HBM in recline postures. Although all of the evaluated HBMs represented the 50th male occupant they showed differing response when tested with matching boundary conditions. At this point it is impossible to evaluate which of the models is closest to the PMHS response since no relevant cadaveric data is available. There are substantial differences in flesh engagement, and pelvis and lumbar spine kinematics between the models, affecting their interaction with the restraint systems. Evaluating the relative biofidelity of these models can only be accomplished with experimental data capturing detailed 3D skeletal kinematics and all the boundary forces necessary for model evaluation.

V. CONCLUSIONS

The following conclusions can be drawn from this study:

- The differences in external body shapes lead to altered lap belt path over the pelvis.
- Out of four HBMs evaluated in recline configuration with matching boundary conditions, the two THUMS models were the most similar, however their response differed from GHBMC-S and GHBMC-D models.
- The GHBMC-D model submarined under the belt, while other models showed good lap belt-pelvis engagement.
- There was a substantial difference in the pelvis and lumbar spine kinematic response between the THUMS and GHBMC models.
- Currently, it is impossible to discriminate between the model responses, since no relevant PMHS data is available.

The HBM are a useful tool for evaluating occupant response in automotive crashes, however they are only applicable within their narrow validation regime. Since the current models were developed to be used in the standard, upright occupant positions, their applicability and validity in the reclined environment remains questionable. Four distinct HBM, developed with the same target, the 50th percentile male occupant, and validated against the same data available from the literature, showed contrasting response when tested in recline scenario. There is a need for additional testing that could be used for development/validation of these models in the recline scenario.

VI. REFERENCES

[1] SAE On-Road Automated Vehicle Standards Committee, (2014) Taxonomy and definitions for terms related to on-road motor vehicle automated driving systems. SAE International.

[2] U.S. Department of Transportation, 2017. Automated Driving Systems 2.0 - A Vision for Safety. Available at: https://www.nhtsa.gov/sites/nhtsa.dot.gov/files/documents/13069a-ads2.0_090617_v9a_tag.pdf Accessed February 21, 2019.

[3] U.S. Department of Transportation, 2017. Automated Driving Systems 3.0 - Preparing for the Future of Transporttation. Available at: https://www.transportation.gov/sites/dot.gov/files/docs/policy-initiatives/automated-vehicles/320711/preparing-future-transportation-automated-vehicle-30.pdf Accessed February 21, 2019.

[4] Martin Östling, M., Larsson, A. (2019) OCCUPANT ACTIVITIES AND SITTING POSITIONS IN AUTOMATED VEHICLES IN CHINA AND SWEDEN, 26th Enhanced Safety of Vehicles, Netherlands, Paper Number 19-0083.

[5]] Jorlöv S., Bohman K., and Larsson A. (2017) Seating Positions and Activities in Highly Automated Cars–A Qualitative Study of Future Automated Driving Scenarios. In Proceedings of IRCOBI conference. Antwerp, Belgium.

[6] Lin, H., Gepner, B., Wu, T., Forman, J., (2018) Effect of Seatback Recline on Occupant Model Response in Frontal Crashes. 2017. Available at: http://www.ircobi.org/wordpress/downloads/irc18/pdf-files/64.pdf. Accessed February 21, 2019.

[7] Gepner, B., Rawska, K., et al., 2019 Challenges for Occupant Safety In Highly Automated Vehicles Across Various Anthropometries. In 26th International Technical Conference on the Enhanced Safety of Vehicles (ESV), In press. 2019. Eindhoven, Netherlands

[8] Rawska, K., Gepner, B., et al., 2019, Submarining Sensitivity across Varied Anthropometry in Autonomous Driving System Environment. Traffic injury prevention, In press

[9] Forman, J., Lin, H., Gepner, B., Wu, T., Panzer, M. (2018) Occupant safety in automated vehicles: effect of seatback recline on occupant restraint. Japan Society of Automotive Engineers.

[10] Kerrigan, J., Rawska, K., et al., 2019, Preventing Submarining for Reclined Occupants of Autonomous Vehicles. Japan Society of Automotive Engineers

[11] Östling, M. Sunnevång, C. Svensson, C. and Kock, H.O. (2017) Potential future seating positions and the impact on injury risks in a Learning Intelligent Vehicle. 11. VDI-Tagung Fahrzeugsicherheit, Nov 29, 2017, Berlin, Germany.

[12] Danelson, K. A., Golman, A. J., Kemper, A. R., Gayzik, F. S., Gabler, H. C., Duma, S. M., Stitzel, J. D. (2015) Finite element comparison of human and Hybrid III responses in a frontal impact. Accident Analysis & Prevention, Volume 85, December 2015, Pages 125-156.

[13] Ji, P., Huang, Y., & Zhou, Q. (2017). Mechanisms of using knee bolster to control kinematical motion of occupant in reclined posture for lowering injury risk. International journal of crashworthiness, 22(4), 415-424.

[14] Richardson, R., Donlon, JP., et al., 2019, Test Methodology For Evaluating The Reclined Seating Environment With Human Surrogates. In 26th International Technical Conference on the Enhanced Safety of Vehicles (ESV), In press. 2019. Eindhoven, Netherlands

[15]Uriot, J., Potier, P., Baudrit, P., Trosseille, X., Petit, P., Richard, O., Compigne, S., Masuda, M. and Douard, R., 2015. *Reference PMHS Sled Tests to Assess Submarining* (No. 2015-22-0008). SAE Technical Paper.

[16]Trosseille, X., Petit, P., Uriot, J., Potier, P., Baudrit, P., Richard, O., Compigne, S., Masuda, M. and Douard, R., 2018. Reference PMHS sled tests to assess submarining of the small female. *Stapp car crash journal*, *62*, pp.93-118.

[17]Schwartz, D., Guleyupoglu, B., Koya, B., Stitzel, J.D. and Gayzik, F.S., 2015. *Development of a computationally efficient full human body finite element model*. Traffic injury prevention, 16(sup1), pp.S49-S56.

[18]Iraeus, J., Pipkorn, B. (2019) Multi-Scale Validation of Rib Strain in Human Body Models. International Research Council on the Biomechanics of Injury (IRCOBI) conference, submitted 2019.

[19]Iwamoto, M., Nakahira, Y. and Kimpara, H., 2015. Development and validation of the total human model for safety (THUMS) toward further understanding of occupant injury mechanisms in precrash and during crash. *Traffic injury prevention*, *16*(sup1), pp.S36-S48.

[20]Nyquist, G.W. and Patrick, L.M., 1976. *Lumbar and pelvic orientations of the vehicle seated volunteer* (No. 760821). SAE Technical Paper.

[21]Gepner, B.D., Joodaki, H., Sun, Z., Jayathirtha, M., Kim, T., Forman, J.L. and Kerrigan, J.R., Performance of the Obese GHBMC Models in the Sled and Belt Pull Test Conditions.

[22]Stemper, B.D., Chirvi, S., Doan, N., Baisden, J.L., Maiman, D.J., Curry, W.H., Yoganandan, N., Pintar, F.A., Paskoff, G. and Shender, B.S., 2018. Biomechanical tolerance of whole lumbar spines in straightened posture subjected to axial acceleration. Journal of Orthopaedic Research®, 36(6), pp.1747-1756.

VII. APPENDIX

APPENDIX A

Modifications to the THUMS v3 model

Body Part		Modification
Chest	**Ribs**	**Geometry and mesh modified** Shi, X., Cao, L., Reed, M. P., Rupp, J. D., Hoff, C. N., Hu, J. (2014) A statistical human rib cage geometry model accounting for variations by age, sex, stature and body mass index. *Journal of Biomechanics,* **47**(10): pp. 2277–85. **Cortical bone thickness modified** Choi, H-Y, Kwak, D-S (2011) Morphologic Characteristics of Korean Elderly Rib. *Journal of Automotive Safety and Energy*, **2**. **Cortical bone properties modified** Kemper, A. R., *et al*. (2005) Material properties of human rib cortical bone from dynamic tension coupon testing. *Stapp Car Crash Journal,* **49**: pp. 199–230. Kemper, A. R., *et al*. (2007) The biomechanics of human ribs: material and structural properties from dynamic tension and bending tests. *Stapp Car Crash Journal,* **51**: pp. 235–73.
	Sternum	**Geometry and mesh modified** 50th percentile male sternum Weaver, A. A., Schoell, S. L., Nguyen, C. M., Lynch, S. K., Stitzel, J. D. (2014) Morphometric analysis of variation in the sternum with sex and age. *Journal of Morphology,* **275**(11): pp. 1284–99.
Lumbar Spine	**Vertebra**	**Remeshed** Contact between vertebra and intervertebral disc added Intervertebral ligaments modified – both geometry and properties Afwerki, H. (2016) Biofidelity Evaluation of Thoracolumbar Spine Model in THUMS. Master's Thesis in Biomedical Engineering, Chalmers University of Technology, 2016.
Head		**New Head Model** Kleiven, S. (2007) Predictors for Traumatic Brain Injuries Evaluated through Accident Reconstructions. *Stapp Car Crash Journal,* **51**: pp. 81–114.

APPENDIX B

GHBMC Lumbar Spine performance curves

Discrete zero length beam lumbar spine performance curves extracted from the GHBMC-S version 1.8.4, and GHBMC-D version 4.5.

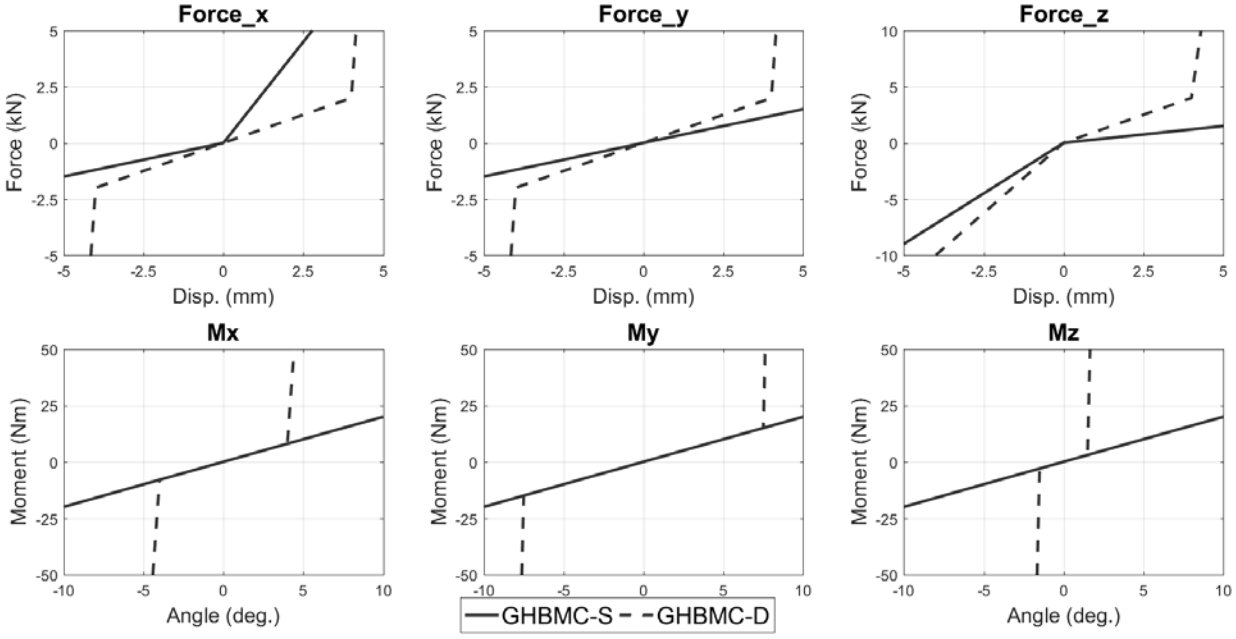

VIII. ERRATUM

Summary

This erratum is intended to address small inconsistency in the results that was discovered after the original manuscript was accepted for publication. All figures affected by the changes are included below in Fig. E 1 through Fig. E 6. No changes within the body of the manuscript were necessary after corrected results were analyzed.

Description of the issue

It has been discovered that for the GHBMC-D model, the numerical slipring located on the D-ring failed to apply a dynamic friction function, thus resulting in a different shoulder belt tension, when compared to other HBMs (Fig. 6). This issue was corrected and the GHBMC-D simulation was repeated. The analysis of the results showed slightly altered kinematics (Fig. E 1, Fig. E 4 and Fig. E 5), belt forces (Fig. E 2), belt trajectories (Fig. E 3), and lumbar spine forces when compared with originally published results.

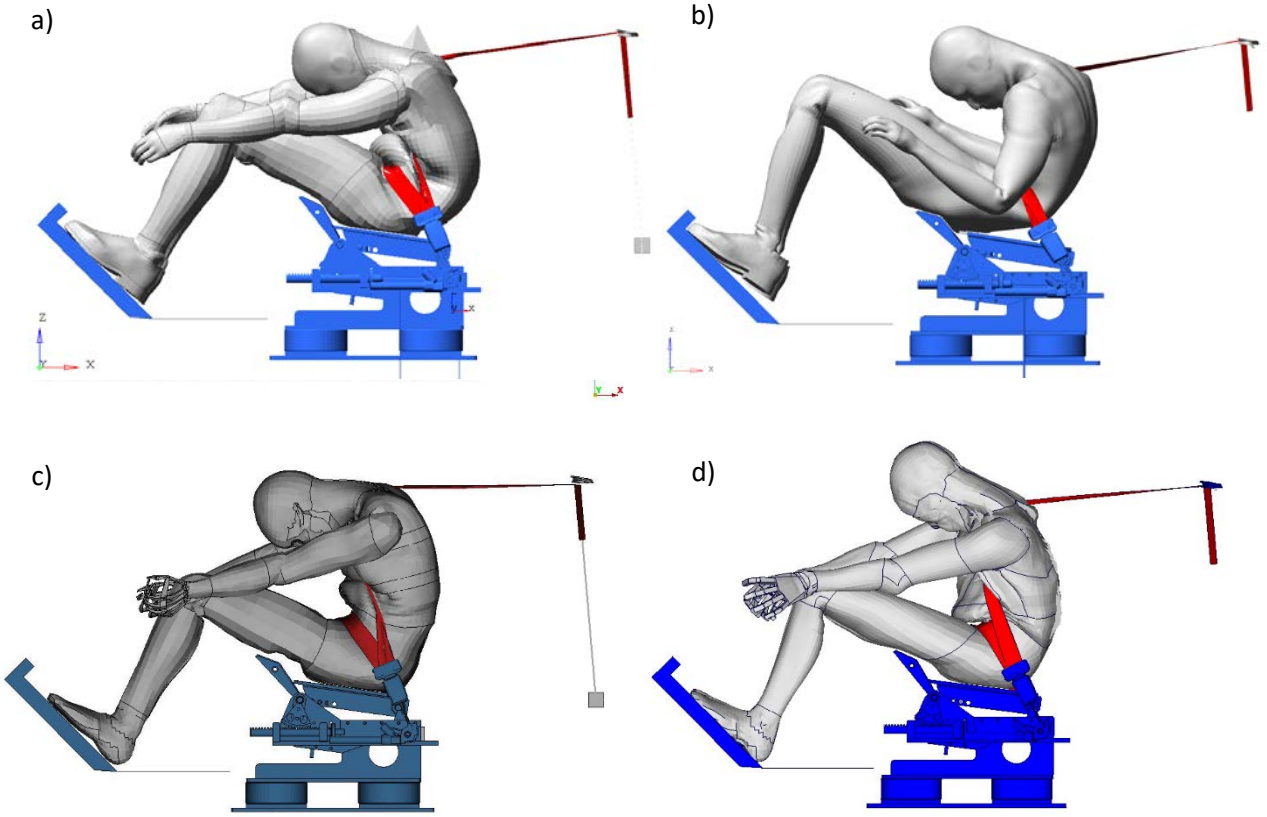

Fig. E 1. Still frames extracted from the simulation at 100 msec. a) GHBMC-S, b) GHBMC-D, c) THUMS-S and d) THUMS-v5.

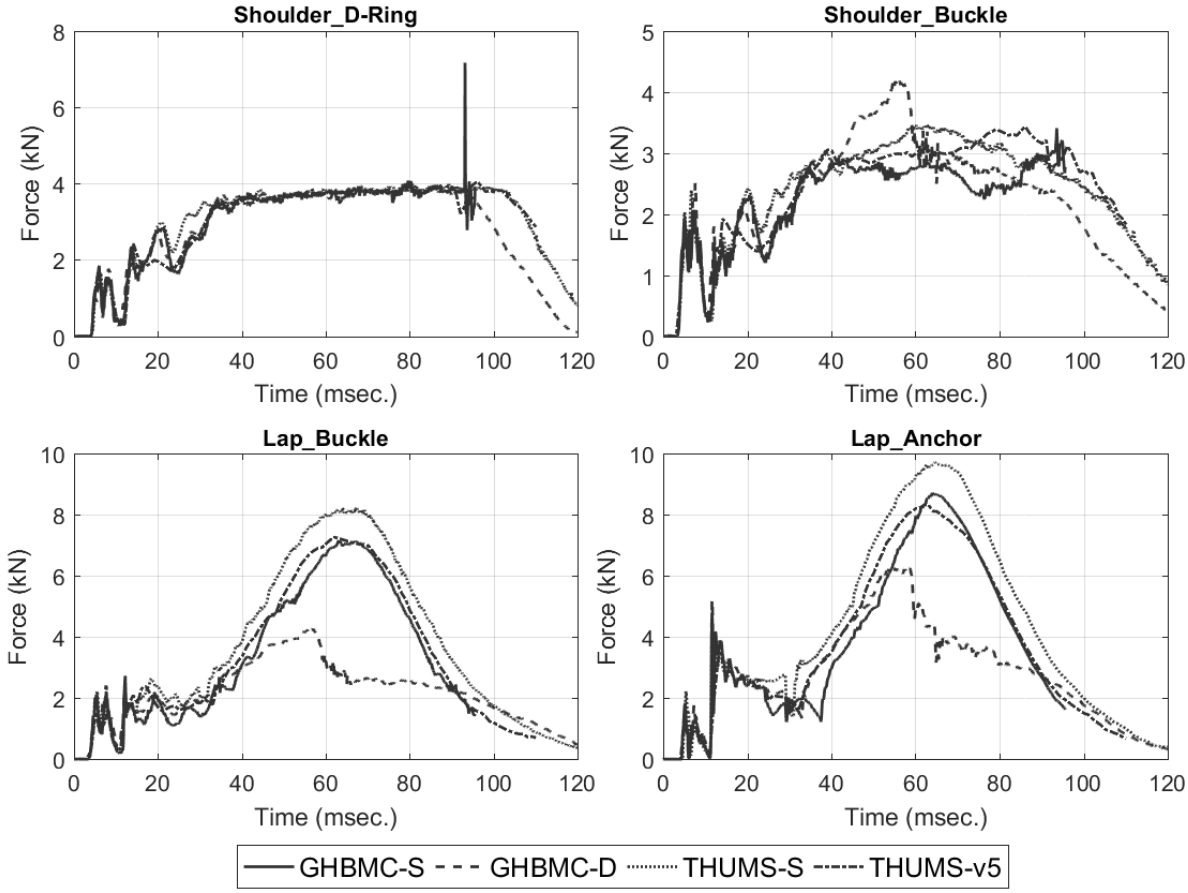

Fig. E 2. Cross-sectional belt forces measured for each HBM.

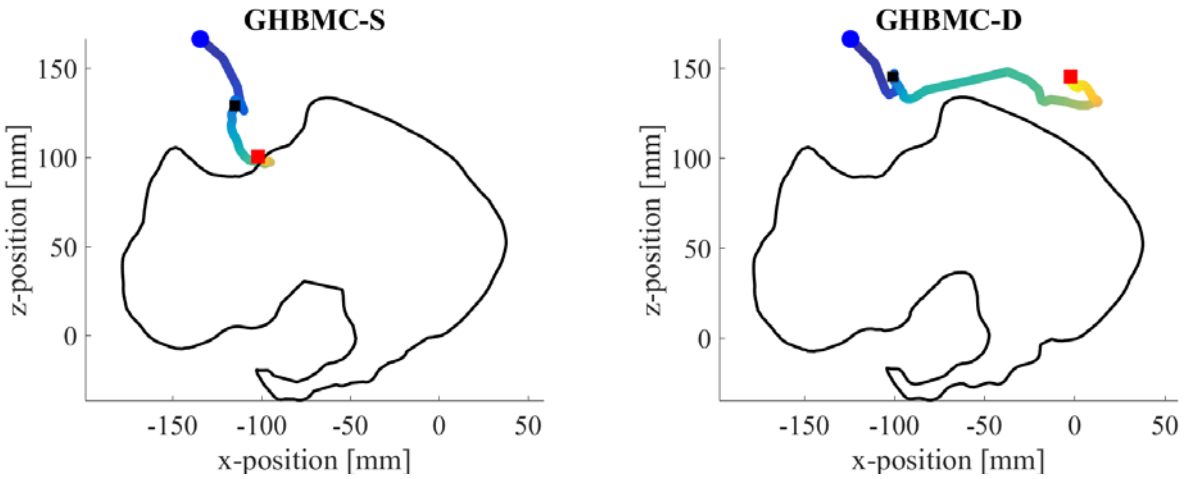

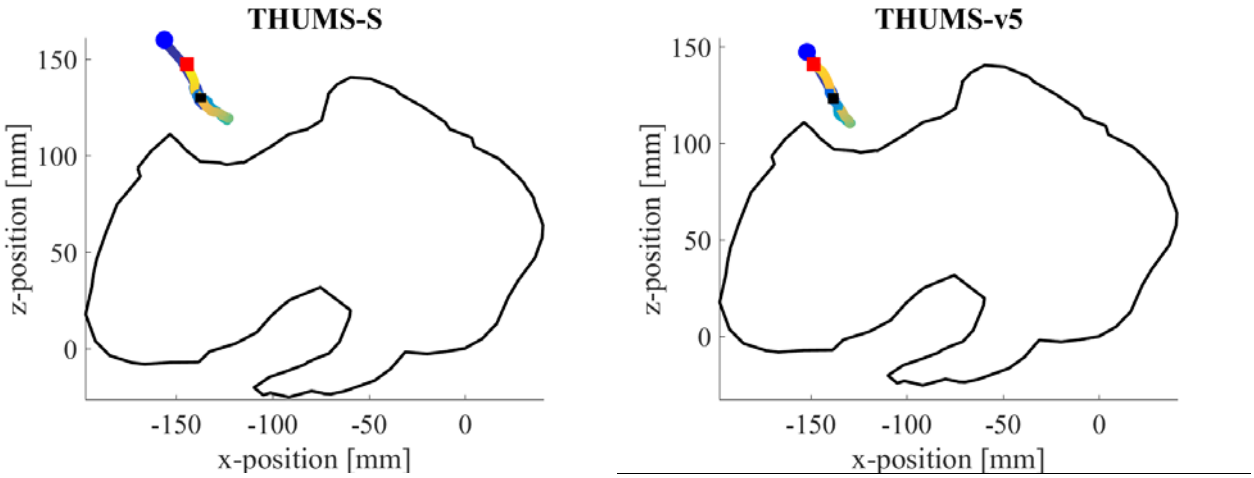

Fig. E 3. Trajectory of the lap belt recorded in the pelvis reference frame. For each case a point at the bottom of the lap belt, directly in front of the left iliac wing is shown. Blue circle depicts the belt initial, and red square its final position. Black square depicts a point (20msec.) after both lap belt pretensiones were fully deployed.

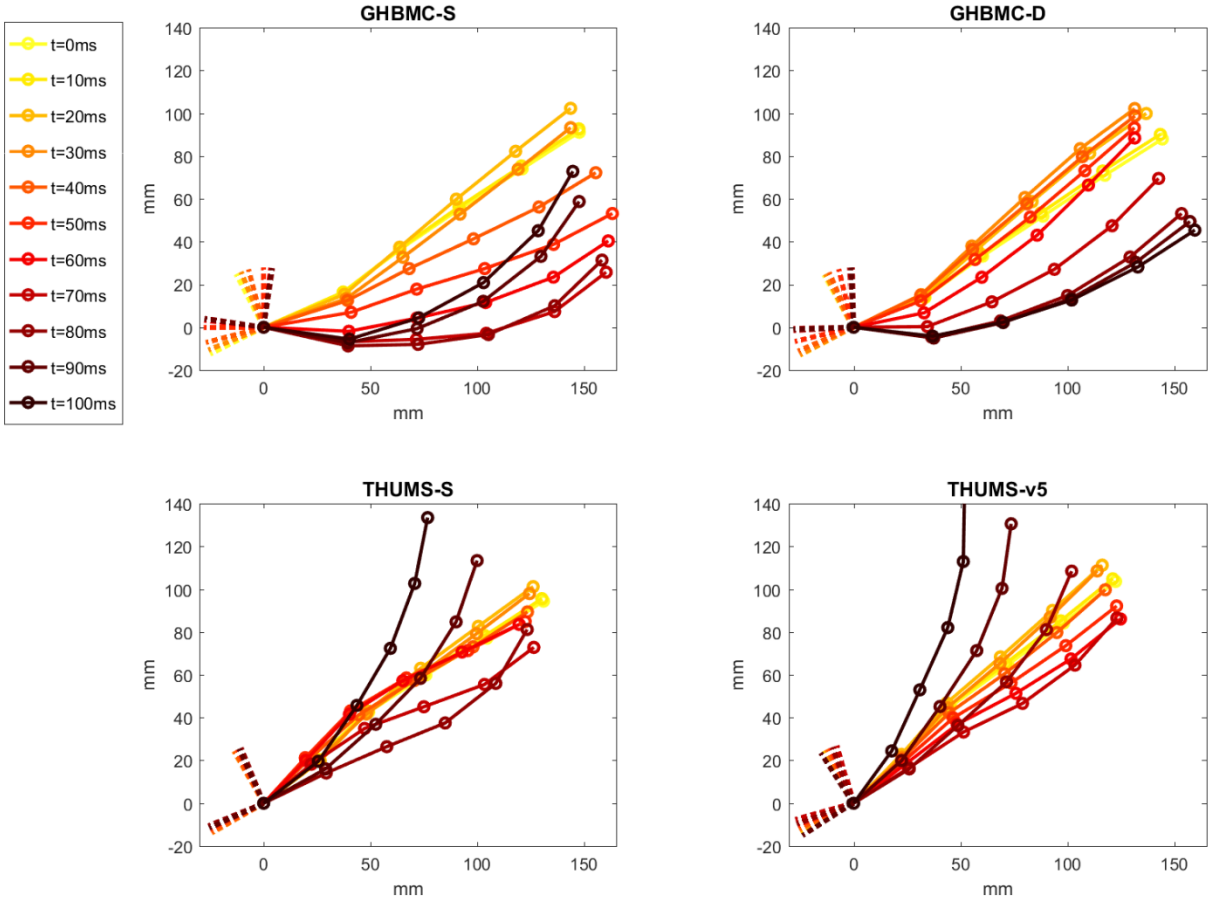

Fig. E 4. Lumbar spine (Pelvis - L1) trajectories across all evaluated HBM. All responses were measured relative to the pelvis origin (Fig. 2). Each vertebra is shown as a dot, and X and Z axis of the pelvis coordinate system are shown as dashed lines.

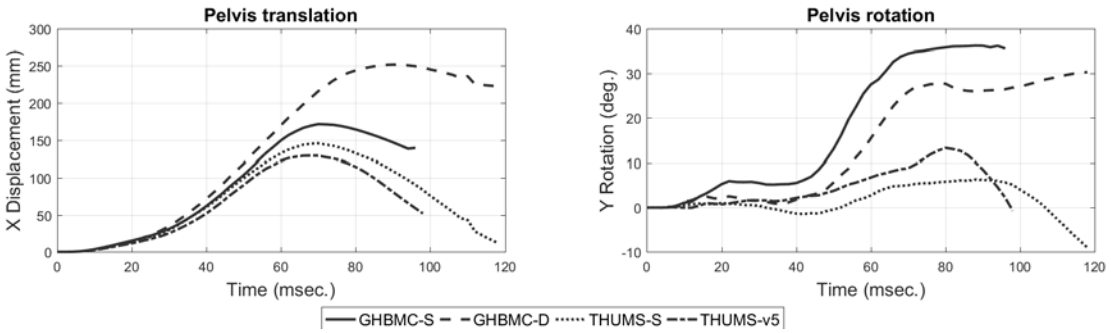

Fig. E 5. Pelvis translation relative to the sled in the longitudinal direction (left), and pelvis rotation in the sagittal plane (right). Comparison across all four evaluated models.

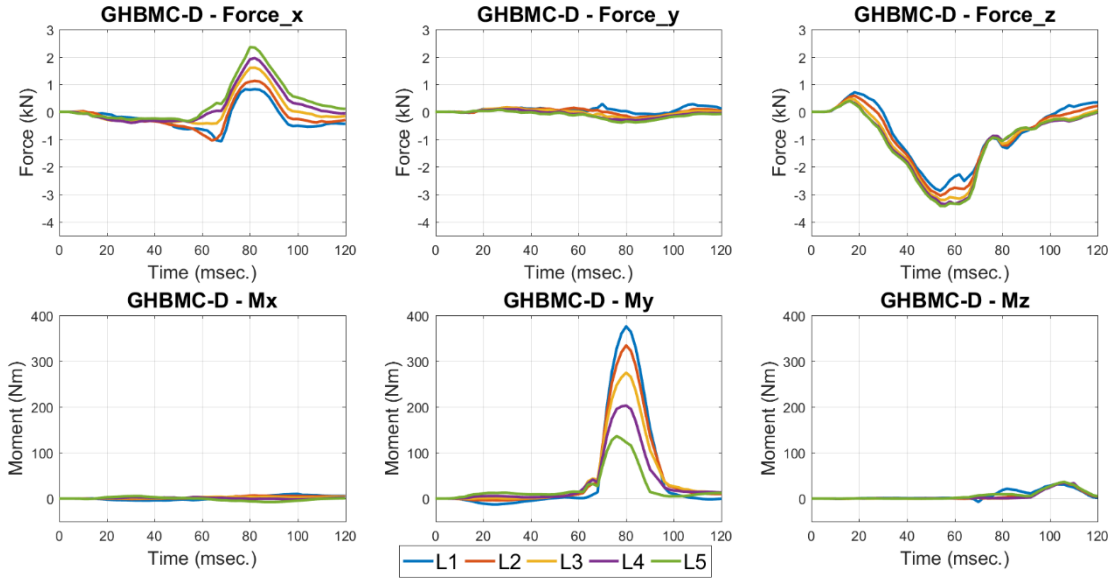

Fig. E 6. Lumbar spine forces recorded for the GHBMC-D model with submarining occuring at 60 msec.